Available online at www.sciencedirect.com
SCIENCE DIRECT®
Journal of Power Sources 129 (2004) 170–179
JOURNAL OF POWER SOURCES
www.elsevier.com/locate/jpowsour

# Effect of a SOFC plant on distribution system stability

Francisco Jurado*, Manuel Valverde, Antonio Cano

*Department of Electrical Engineering, University of Jaén, 23700 EUP Linares, Jaén, Spain*

Received 21 February 2003; accepted 3 November 2003

**Abstract**

When connected in small amounts, the impact of distributed generation (DG) on distribution system stability will be negligible. However, if its penetration level becomes higher, distributed generation may start to influence the dynamic behavior of the system as a whole. This paper presents a mathematical representation of a solid oxide fuel cell plant that is suitable for use in distribution system stability studies. The model is applied to a distributed utility grid that uses a solid oxide fuel cell plant as distributed resource. Examinations include transient stability and voltage stability of the system.


*Keywords:* Distributed generation; Power system dynamic stability; Solid oxide fuel cell (SOFC); Transient stability

## 1. Introduction

Distributed generation (DG) is electricity generation sited close to the load it serves, typically in the same building or complex. The DG embraces a palette of technologies in varying stages of availability, from entrenched to pilot. It is sometimes called a "disruptive" technology because of its potential to upset the utility industry's apple cart.

Most likely, fuel cells will be a dominant DGs [1,2]. These DGs are dynamic devices and when connected to the distribution system they will affect its dynamic behavior. Hence, several researchers are working to develop dynamic models for these components [3–10].

This paper develops a generic dynamic model for a grid-connected SOFC plant. The model is defined by a small number of parameters and is suitable for planning studies.

The steady-state power generation characteristics of the plant are derived and analyzed. Understanding the transient behavior of SOFC is important for control of stationary utility generators during power system faults, surges and switchings.

Voltage regulation is one of the main problems in the distribution systems, especially at the much far-end load and in the rural areas. Voltage regulation and maintaining the voltage level are well-known problems in the radial distribution network. Several techniques have been applied by implementing many devices in the distribution network to solve these problems. The most common devices and techniques used are transformer equipped by load tap changer, supplementary line regulators installed on distribution feeders, shunt capacitor switched on distribution feeders [11] and shifting transformers towards the load center [12]. A multiple line drop compensation voltage regulation method that determines tap positions of under-load tap changer transformers is proposed in [13] to maintain the customers' voltages within the permissible limits.

The model derived is based on the main equations. It is developed in the Laplace domain and transient simulation is done using a software developed based on the MATLAB package.

The paper is structured as follows. Section 2 presents a review of transient stability. Some basic concepts of voltage stability are introduced in Section 3. Section 4 describes the SOFC model. Section 5 briefly discusses the utility-connected inverter control. Section 6 depicts some simulation results. Finally, conclusions are presented in Section 7.

## 2. Transient stability

Transient stability is a term applied to alternating current (ac) electric power systems, denoting a condition in which the various synchronous machines of the system remain in synchronism, or in step each other. Conversely, instability denotes a condition involving loss of synchronism, or falling out of step [14].

* Corresponding author. Tel.: +34-953-026518; fax: +34-953-026508.
*E-mail address:* fjurado@ujaen.es (F. Jurado).

0378-7753/$ – see front matter © 2003 Elsevier B.V. All rights reserved.
doi:10.1016/j.jpowsour.2003.11.001

**Nomenclature**

*Fuel cell*

| | |
|---|---|
| $E_0$ | ideal standard potential |
| $F$ | Faraday's constant |
| $I_{fc}$ | fuel cell current |
| $K_{H_2}$ | valve molar constant for hydrogen |
| $K_{H_2O}$ | valve molar constant for water |
| $K_{O_2}$ | valve molar constant for oxygen |
| $K_r$ | constant, $K_r = N_0/4F$ |
| $N_0$ | number of cells in series in the stack |
| $P$ | real power |
| $P^*$ | set point for the real power |
| $p_i$ | partial pressure |
| $q_{fc}^{in}$ | input fuel flow |
| $q_{fc}^{r}$ | fuel flow that reacts |
| $r$ | ohmic loss |
| $r_{H-O}$ | ratio of hydrogen to oxygen |
| $R$ | universal gas constant |
| $T$ | absolute temperature |
| $T_e$ | electrical response time |
| $T_f$ | fuel processor response time |
| $U$ | fuel utilization |
| $V_{fc}$ | fuel cell voltage |
| $\tau_{H_2}$ | response time for hydrogen flow |
| $\tau_{H_2O}$ | response time for water flow |
| $\tau_{O_2}$ | response time for oxygen flow |

*Inverter*

| | |
|---|---|
| $\boldsymbol{E}$ | load bus voltage |
| $\boldsymbol{E}^*$ | set point for the load bus voltage |
| $L_T$ | inductance |
| $Q$ | reactive power |
| $Q^*$ | set point for the reactive power |
| $\boldsymbol{V}$ | inverter output voltage space vector |
| $X_T$ | reactance $= L_T\omega$ |
| $\delta_p$ | angle between $\psi_v$ and $\psi_e$ |
| $\delta_p^*$ | angle reference |
| $\delta_p^*$ | flux vector associated with $\boldsymbol{V}$ |
| $\psi_e$ | flux vector associated with $\boldsymbol{E}$ |
| $\psi_v^*$ | flux-vector reference |

*Distribution network stability*

| | |
|---|---|
| $D_x f$ | system Jacobian |
| $H$ | inertia constant |
| $P_e$ | electrical power output, in p.u. |
| $P_i$ | initial load |
| $P_L$ | active load at a bus |
| $P_m$ | mechanical power, in p.u. |
| $P_{nL}$ | load distribution factor |
| $P_0$ | active power base load |
| $\boldsymbol{x}$ | state variables |
| $\Delta P_L$, $\Delta Q_L$ | changes in load demand |
| $\delta$ | rotor angle, in electrical radian |
| $\lambda$ | changes in the system loading |
| $\omega_0$ | nominal speed, in electrical rad/s |

Hence, for a simplified intuitive description of transient stability, a power system may be regarded as a set of synchronous machines and of loads interconnected through the transmission network. Under normal operating condition, all the system machines run at the synchronous speed. If a large disturbance occurs the machines start swinging with respect to each other, their motion being governed by differential equations. Depending upon the power system modeling, the number of such first-order differential equations is lower bounded by twice the number of system machines, but may be orders of magnitude larger.

DG units normally supply power to the local load centers but the excess power could also be exported to the regional power grid, adding to the capacity and stability of the grid system.

The key to interconnection is the safety of the people who have to clear faults on the line, and protecting the DG generator from feeding into a low-impedance fault. A fault will knock DG off the system, requiring it to be resynchronized with the grid. There are various means to enhance the transient stability performance of the distribution systems [15–17].

Fast valving is one of the most effective and economic means of improving the stability of a power system under large and sudden disturbances. Fast valving schemes involve rapid closing and opening of thermal turbine valves in a prescribed manner to reduce the generator acceleration following a severe fault [18].

During steady-state operation of a power system, there is equilibrium between the mechanical input power of each unit and the sum of losses and electrical power output of that unit. The problem arises when there is a sudden change in the electrical power output due to a severe and sudden disturbance. The severity is measured by drop of this power to a very low or to zero value and a consequential sudden acceleration of the machines governed by the swing equation:

$$\frac{2H}{\omega_0}\frac{\mathrm{d}^2\delta}{\mathrm{d}t^2} = P_m - P_e \tag{1}$$

where $\delta$ is the rotor angle, in electrical radian, $P_m$ the mechanical power, in p.u., $P_e$ the electrical power output, in p.u., $H$ the inertia constant, in MW s/MVA, $\omega_0$ the nominal speed, in electrical rad/s.

From (1), it is apparent that the decrease in the mechanical power has the same impact on the rotor angle swings as that of increase in the electrical power output. Fast valving has a function of reducing the mechanical power input to the turbine and so the generated power.

A change in load demand ($\Delta P_L$, $\Delta Q_L$) causes corresponding change in both bus voltage magnitude and the power output of the generator. The voltage magnitude value is calculated in the power flow analysis. The change in the generator's active power output results in system frequency variations through the swing equations.

## 3. Voltage stability

Voltage instability spans a range in time from a fraction of second to tens of minutes. Time response charts have been used to describe dynamic phenomena [19,20]. Many electric system components and controls play a role in voltage stability. Only some, however, will significantly participate in a particular incident or scenario. The system characteristics and the disturbance will determine which phenomena are important.

### 3.1. Mid-term voltage stability

The time frame is several minutes, typically 2–3 min. Operator intervention is often not possible. This scenario involves high loads, and a sudden large disturbance. The system is transiently stable because of the voltage sensitivity of loads. The disturbance (loss of generators in a load area or loss of major distribution lines) causes high reactive power losses and voltage sags in load areas.

### 3.2. Longer-term voltage stability

The instability evolves over a still longer time period and is driven by a very large load buildup, or a large rapid power transfer increase. The load buildup, measured in MW/min, may be quite rapid.

Several papers have shown the direct relation between saddle-node bifurcations and voltage collapse problems, e.g. [21,22]. Saddle-node bifurcations, also known as turning points, are generic codimension one local bifurcations of nonlinear dynamical systems of the form

$$\frac{\mathrm{d}x}{\mathrm{d}t} = f(x, \lambda) \tag{2}$$

where $\boldsymbol{x} \in R^n$ are the state variables, $\lambda \in R$ is a particular scalar parameter that drives the system to bifurcation in a quasi-static manner, and $f$: $R^n \times R \rightarrow R^n$ is a nonlinear function. System exhibits a saddle-node bifurcation at the equilibrium point $(\boldsymbol{x}_0, \lambda_0)$, i.e., $f(\boldsymbol{x}_0, \lambda_0) = 0$, if the corresponding system Jacobian $D_x f|_0 = D_x f(\boldsymbol{x}_0, \lambda_0)$ has a unique zero eigenvalue, and some particular transversality conditions hold at that equilibrium point.

The state variables $\boldsymbol{x}$ and nonlinear function $f(.)$ are typically defined in terms of the quasi-steady state phasor models used in transient stability studies. Thus, generator angular speed deviations and phasor bus voltages, magnitudes and angles, are usually an important part of vector $x$. The parameter $\lambda$ is typically used to represent changes in the system loading, regardless of the load model used.

Therefore, typically one starts from an initial stable operating point and increases the constant power loads by a factor $\lambda$, until the singular point of the linearization of the power flow equations is reached. The loads can be defined as:

$$P_{\mathrm{L}} = P_0(1 + \lambda P_{n\mathrm{L}}) \tag{3}$$

where $P_0$ is the active power base load, $P_{n\mathrm{L}}$ represents the load distribution factor and $P_{\mathrm{L}}$ the active load at a bus $L$ for the current operating point.

## 4. Solid oxide fuel cell

There are several types of fuel cells being developed for a variety of applications and these have been extensively discussed in the open literature. Unlike other variants, the SOFC is entirely solid state with no liquid components. Operation at elevated temperature is needed to achieve the necessary level of conductivity in the cell's solid electrolyte for it to operate efficiently. With an outlet temperature in the range of 900–1000 °C, the efficiency of the cell alone is about 50%.

Typically the fuel cell system consists of SOFC generator modules in a parallel flow arrangement, with the number of standard modules being determined by the plant power requirement. The SOFC generator module embodies a number of tubular cells, which are combined to form cell bundle rows, several of which are arranged side by side to make up the complete assembly.

The high efficiency of the system means that less carbon dioxide is generated than in contemporary power plants. In addition, the fuel is oxidized electrochemically without any interaction with atmospheric nitrogen so negligible amounts of nitrogen oxide are discharged to the environment.

This paper provides a basic SOFC power section dynamic model used for performance analysis during normal operation. Some control strategies of the fuel cell system, response functions of fuel processor and power section are combined to model the SOFC power generation system.

The chemical response in the fuel processor is usually slow. It is associated with the time to change the chemical reaction parameters after a change in the flow of reactants. This dynamic response function is modeled as a first-order transfer function with a 5 s time constant.

The electrical response time in the fuel cells is generally fast and mainly associated with the speed at which the chemical reaction is capable of restoring the charge that has been drained by the load. This dynamic response function is also modeled as a first-order transfer function but with a 0.8 s time constant.

With aid of the inverter, the fuel cell system can supply not only real power but also reactive power. Usually, power factor can be in the range of 0.8–1.0. The SOFC system dynamic model is given in Fig. 1.

### 4.1. Instantaneous power issue

The introduction of a micro-source within an existing power system assumes that there may be a cluster of small generators located in electrical proximity, interconnected through on-site feeders and operation can be isolated or connected to a distribution grid.

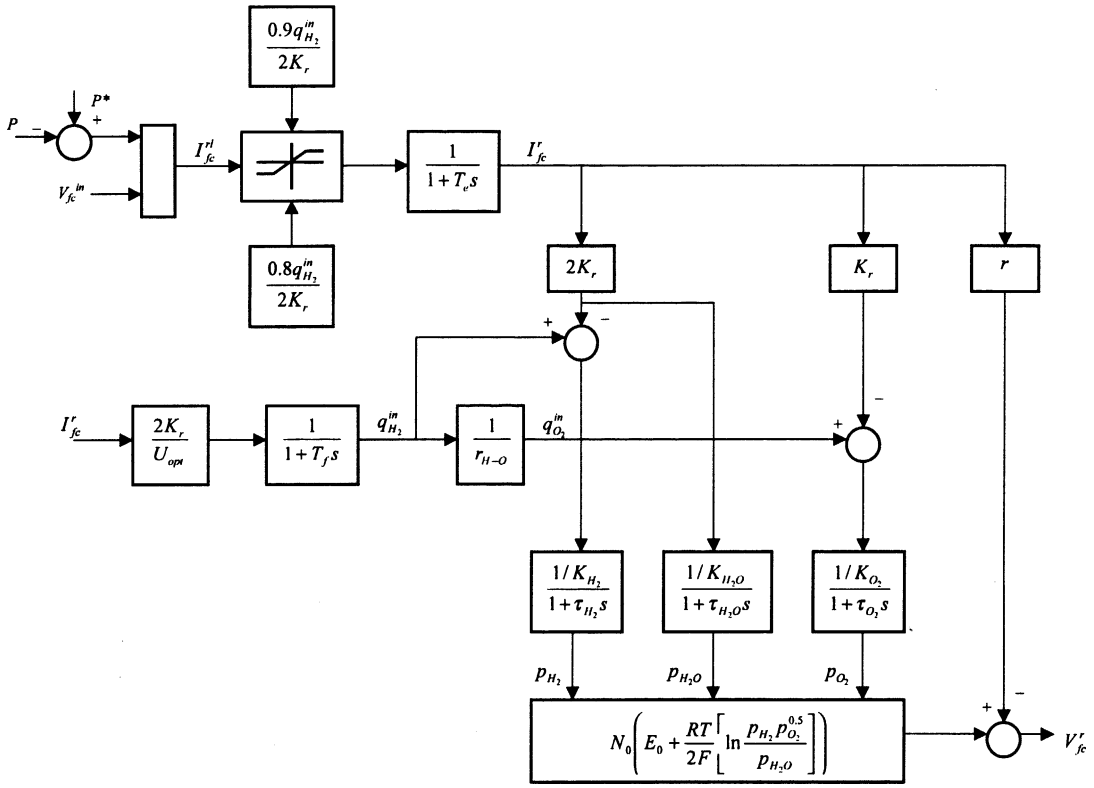


Fig. 1. SOFC system dynamic model.

SOFCs have a slow response to changes in commands and also do not provide any kind of internal form of energy storage. These inertia-less systems are not well suited to handle step changes in the requested output power. It must be remembered that the current power systems have storage in the mechanical energy of the inertia of the generators. When a new load is applied the initial energy balance is satisfied by the inertia of the system, this results in a slight reduction in system frequency.

The step sized power demand in the distribution system should be instantaneously matched by an identical supply of power from the micro-source power source.

### 4.2. Load coming on-line with grid connection

SOFCs have a problem in instantaneous power tracking. SOFC shows a poor load tracking, as a load is applied and the micro-source ramps up to pick up the whole quota of extra power request. The missing transient power that the micro-source is not fast enough to provide is taken from the connection with the grid that supplies only a part of the local requested power during steady-state. Voltage is maintained by the power grid.

### 4.3. Load coming on-line without grid connection

The requested power from the load coming on-line is a step function, while the inertia-less micro-source always takes a finite amount of time to ramp up to the newly requested value. Since the unit cannot change its output power instantaneously, the power is balanced by voltage reduction. As the power injected from the micro-source increases to supply the needed load the voltage is restored.

There is a missing quota of energy from the difference of the power that the load is requesting and the power that the unit is able to provide. If the connection to the main grid is active, then the missing quota can be provided by the utility. It will be seen from the grid terminals as a temporary, pulse-like power request.

## 5. Utility-connected inverter control

For a six-pulse voltage source inverter, the inverter output voltage space vector can take any of seven positions in the plane specified by the *d*–*q*-coordinates. The time integral of the inverter output voltage space vector is called the “inverter flux vector” for short. The flux vector does not have the same significance as in motor applications. Rather, it is a fictitious quantity related to the volt-seconds in the filter inductor [23]. The *d*- and *q*-axes components of the inverter flux vector $\psi_v$ are defined as:

$$\psi_{dv} = \int_{-\infty}^{t} v_d \, d\tau \tag{4}$$

$$\psi_{dq} = \int_{-\infty}^{t} v_q \, d\tau \tag{5}$$

The magnitude of $\psi_v$ is

$$|\psi_v| = \sqrt{\psi_{qv}^2 + \psi_{dv}^2} \tag{6}$$

The angle of $\psi_v$ with respect to the $q$-axis is:

$$\delta_v = \tan^{-1}\left(\frac{-\psi_{dv}}{\psi_{qv}}\right) \tag{7}$$

The $d$- and $q$-axes components of the ac system voltage flux vector $\psi_e$, its magnitude, and angle are defined in a similar manner. The angle between $\psi_v$ and $\psi_e$ is defined as:

$$\delta_p = \delta_v - \delta_e \tag{8}$$

Control of the flux vector has been shown to have good dynamic and steady-state performance. It also provides a convenient means to define the power angle since the inverter voltage vector switches position in the $d$–$q$-plane, whereas there is no discontinuity in the inverter flux vector.

It is useful to develop the power transfer relationships in terms of the flux vectors. The basic real power transfer relationship for the control system of Fig. 2 in the $d$–$q$ reference frame is:

$$P = \tfrac{3}{2}(e_q i_q + e_d i_d) \tag{9}$$

In (9), $e_q$ and $e_d$ are the $q$- and $d$-axes components, respectively, of the ac system voltage vector $\boldsymbol{E}$. In addition, $i_q$ and $i_d$ are the components of the current vector $\boldsymbol{I}$. When $i_q$ and $i_d$ are expressed in terms of the fluxes, the equation is expressed as:

$$P = \frac{3}{2L_T}[e_q(\psi_{qv} - \psi_{qe}) + e_d(\psi_{dv} - \psi_{de})] \tag{10}$$

Taking into account the spatial relationships between the two flux vectors and assuming the ac system voltage to be sinusoidal, (10) can be expressed as:

$$P = \frac{3}{2L_T}\omega\psi_e\psi_v \sin\delta_p \tag{11}$$

In this expression, $\psi_e$ and $\psi_v$, are the magnitudes of the ac system and the inverter flux vectors, respectively, and $\delta_p$ the spatial angle between the two flux vectors. $\omega$ is the frequency of rotation of the two flux vectors. The expression for reactive power transfer can be derived in a similar manner. This is

$$Q = \frac{3\omega}{2L_T}[\psi_e\psi_v \cos\delta_p - \psi_e^2] \tag{12}$$

Eqs. (11) and (12) indicate that $P$ can be controlled by controlling $\delta_p$, which can be defined as the power angle, and $Q$ can be controlled by controlling $\psi_v$. The cross coupling between the control of $P$ and $Q$ is also apparent from these equations.

The two variables that are controlled directly by the inverter are $\psi_v$ and $\delta_p$. The vector $\psi_v$ is controlled to have a

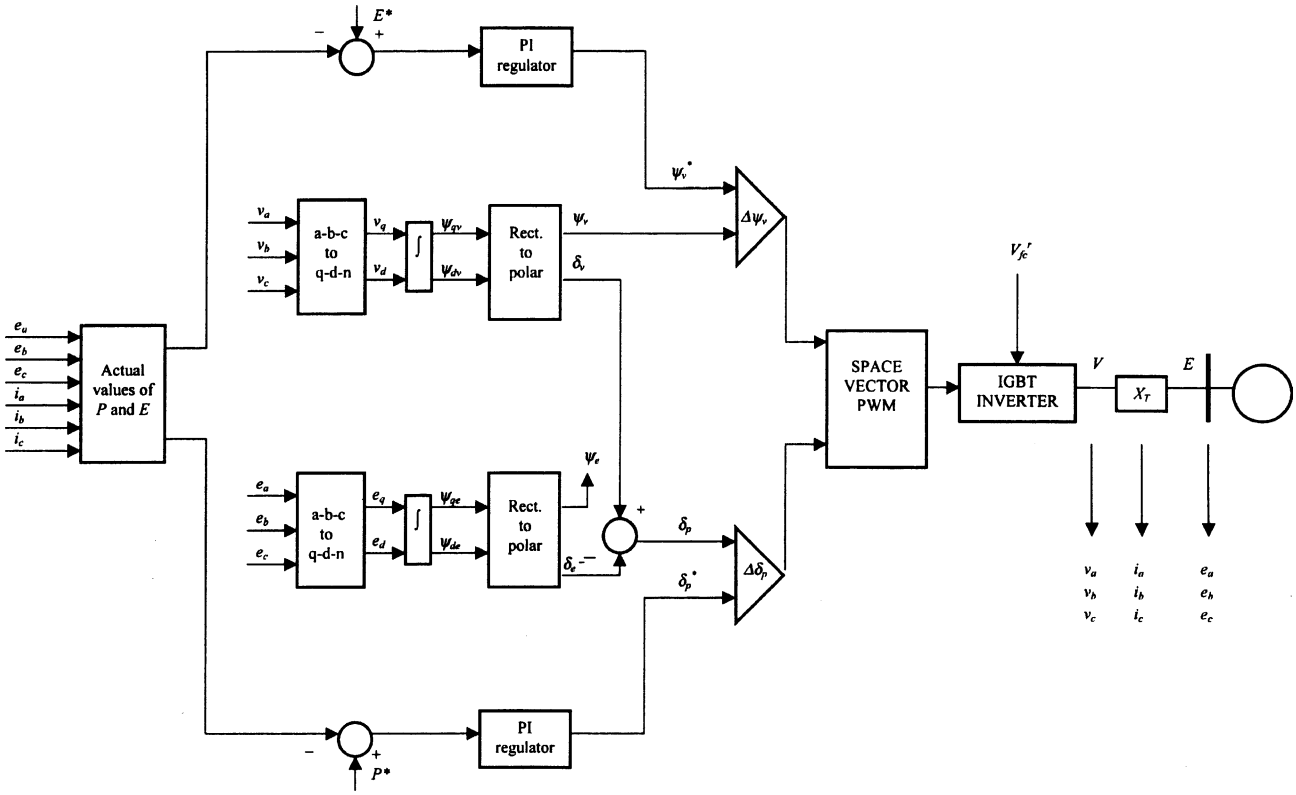


Fig. 2. Control system for the inverter.

specified magnitude and a specified position relative to the ac system flux vector $\psi_e$. This control forms the innermost control loop and is very fast. It is noted that both the inverter and the ac system voltage space vectors are obtained by measuring instantaneous voltage values that are available locally. The set points for the controller are $P^*$ and $E^*$, and the set points for the innermost control loop $\psi_v^*$ and $\delta_p^*$ are derived from these.

The actual values of $P$ and $E$ calculated from the feedback are compared with the set values. The error drives a proportional integral (PI) regulator, which generates the set points $\psi_v^*$ and $\delta_p^*$ for the innermost control loop.

The errors between actual and desired amounts activate the remainder of the firing scheme only if they exceed a threshold value. If the error is larger than the hysteresis band (whose widths are $\delta_p^*$ and $\psi_v^*$) then a decision towards a new switching sequence is made. If the errors are within their hysteresis band, the switches will hold their current status.

The new switching position is chosen according to the current angular position of the vector at the inverter terminals defined by $\delta_v$, and depending on the fact that we need to increase/decrease the flux magnitude or its angle. Angle changes have priority on flux magnitude changes. Once the hysteresis threshold is crossed and the direction of the next switching is selected, a lookup table will give the gating sequence for the switches.

Therefore, the SOFC plant has two major control loops:

1. Power control: done by adjusting the set point $P^*$ of the inverter for fast transient variations and fuel flow input control for slow variations.
2. Voltage control: done by adjusting the set point $E^*$ of the inverter, which effects the magnitude of the converter output voltage.

Using the fast response of the inverter, the maximum power can be used to alleviate transients when fault occurs. However, the inverters for fuel cells have the following limitations:

- Overused fuel, $U > 90\%$ (fuel starvation and permanent damages to cells).
- Underused fuel, $U < 70\%$ (the cell voltage would rise rapidly).
- Undervoltage, stack voltage < certain point (loss of synchronism with the network).

Where, the fuel utilization ($U$) is the ratio between the fuel flow that reacts and the input fuel flow, such as the follows:

$$U = \frac{q_{H_2}^{in} - q_{H_2}^{o}}{q_{H_2}^{in}} = \frac{q_{H_2}^{r}}{q_{H_2}^{in}} \quad (13)$$

## 6. Results

The analysis is tested on a system consists of 13 buses and is representative of a medium-sized industrial plant. The system is shown in Fig. 3 and described by the data in Table 1.

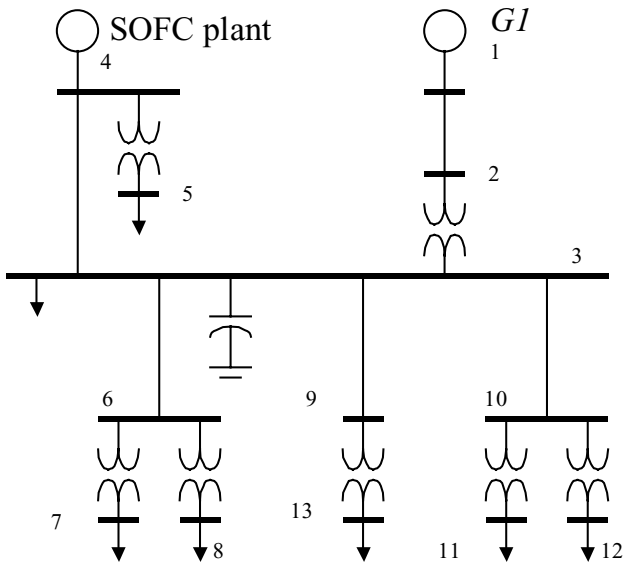


Fig. 3. Test system.

The SOFC plant is connected at bus 4 and consists of 20 SOFCs, as depicted in Fig. 3. The majority of data for the fuel cell model has been extracted from [24,25], and a commercial leaflet describing a SOFC 100 kW plant. Each SOFC has the same parameters, yielding a rated power of 2 MW.

Suppose at a certain time, the total load in this distribution system is as shown in Table 1. The SOFC plant mainly provide some peak shaving capability and ancillary services for the feeder.

It is assumed bilateral contracts to perform load-following among SOFCs at a given feeder is not allowed. That is, the ancillary service must be coordinated at the substation or transmission level.

It is desirable to minimize the number of dynamic equations to be solved in the simulations. Here, all SOFCs in the

Table 1
Generation, load, and bus voltage data, base case

| Bus | $V_{mag}$ (%) | $P_{gen}$ (kW) | $Q_{gen}$ (kvar) | $P_{load}$ (kW) | $Q_{load}$ (kvar) |
|---|---|---|---|---|---|
| 1 | 100.00 | 7450 | 540 | – | – |
| 2 | 99.89 | – | – | – | – |
| 3 | 99.59 | – | – | 2240 | 2000 |
| 4 | 99.64 | 2000 | 1910 | – | – |
| 5 | 101.88 | – | – | 600 | 530 |
| 6 | 99.56 | – | – | – | – |
| 7 | 101.94 | – | – | 1150 | 290 |
| 8 | 104.06 | – | – | 1310 | 1130 |
| 9 | 99.56 | – | – | – | – |
| 10 | 99.52 | – | – | – | – |
| 11 | 99.31 | – | – | 370 | 330 |
| 12 | 103.30 | – | – | 2800 | 2500 |
| 13 | 101.64 | – | – | 810 | 800 |

plant are regarded as coherent devices, which have the same dynamic response and share the generation equally.

### 6.1. Step change response

A power measurement is fed in the fuel flow regulator, whose output determines the position of a fuel valve. A step change in the input reactant element will not be noticed as a sudden increase in charges. Typically, there is a sudden but contained rise in output power that takes place in 1–3 s, while the newly desired output power level is reached limited until the SOFC reaches its thermal equilibrium, which may tens of seconds. This characteristic makes the SOFC a poor candidate for isolated systems, where loads require instantaneous power.

Assume a SOFC is operating with constant rated voltage and power demand ($P_L$) 0.6 p.u. There is 0.3 p.u. of step increase in the total load at $t = 10$ s. In the first 2 s or 3 s after $P_L$ is increased, $P$ has a rapid increase due to the fast electrical response time in the fuel cell. Subsequently, $P$ increases slowly and continuously until reaching the required power. This is due to the slow chemical response time in the fuel processor. The total response time of $P$ from 0.6 to 0.9 p.u. is about 30 s. Fig. 4 shows the response of the SOFC to a step change in the fuel valve.

Normally the fuel cell supports base load thus, the fuel flow regulator in Fig. 1 is set to provide a constant input flow-rate for the cell fuel. The response of the fuel flow regulator is slow. The plant, however, can respond continuously to small instantaneous power adjustment by the control of the angle $\delta_p^*$. Any steady-state power change must be followed by a corresponding change in the fuel flow-rate. If the fuel cell power increases while the fuel flow-rate is maintained constant, the steady-state cell utilization will increase and the cell voltage will drop.

### 6.2. Transient stability

Penetration means the proportion of the distribution load being supplied by SOFC plant [26]. In this model, an initial load of $P_i$ is assumed and the penetration is thus,

$$\text{penetration} = \frac{P}{P + P_i} \tag{14}$$

for this reason, the penetration level of this SOFC plant is set at 20%.

A faults occurs that disconnects the utility supply from the distribution system. The fault clearing is after 0.4 s. The comparison between Figs. 5 and 6 show the advantage of a fast power controller. Since the SOFC inverter has the capability to adjust its angle $\delta_p^*$ quickly, the inverter maintains constant power output under fast transient disturbances. In addition, SOFC inverter has power modulation capabilities that enhance transient stability of the system.

### 6.3. Voltage stability

This section discusses the nature of the response of system to a linear increase in load demand. In the load flow calculation, SOFC plant is considered as a PV bus where $P$ and $E$ (shown in Fig. 2) are specified.

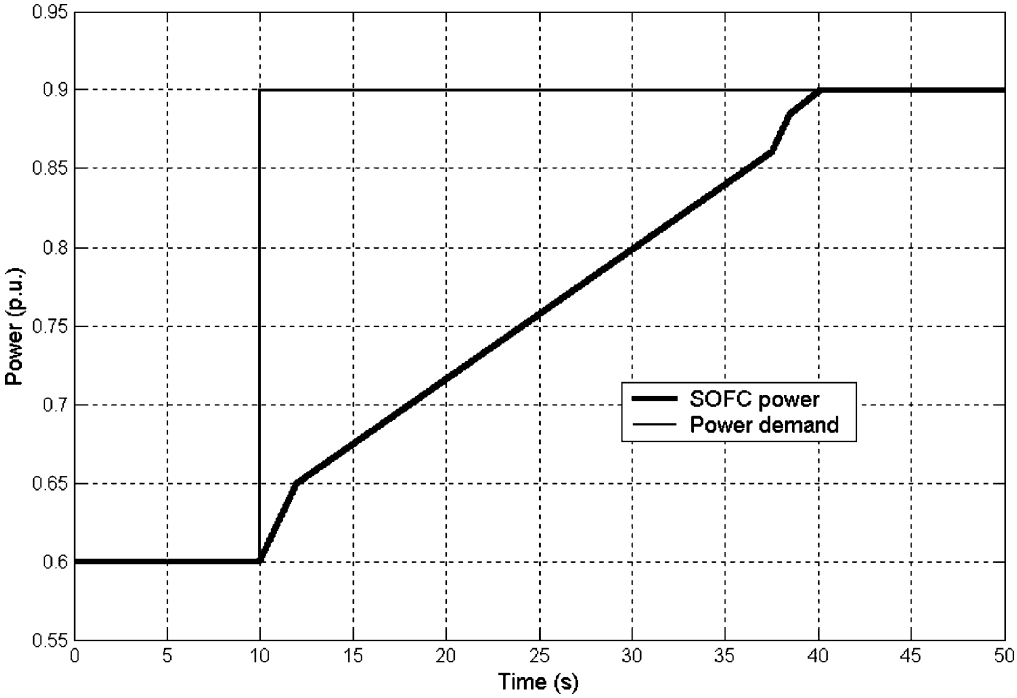


Fig. 4. SOFC plant response to a step change in the power demand.

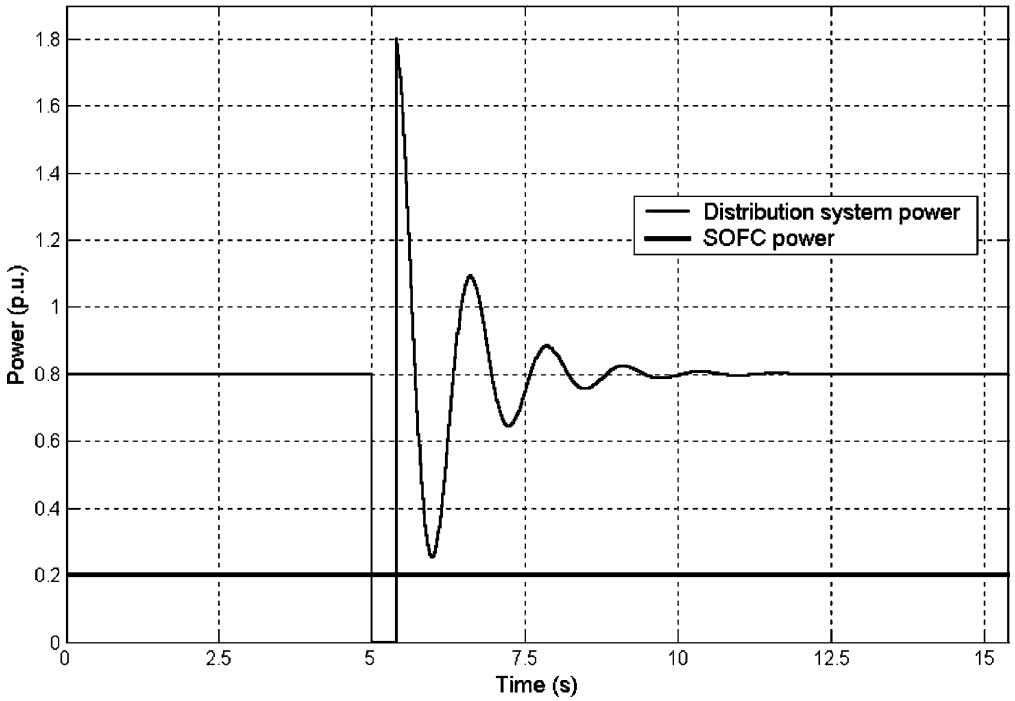


Fig. 5. Fast transient disturbances without inverter.

The power load $P_L$ increases by a factor until the voltage collapse is reached. The analysis is tested on the distribution system. Continuation method is used to identify the location of bifurcation point ($\lambda = 2.45$), as presented in Fig. 7.

Fig. 8 displays the output power for the SOFC. Simulation times are 180 s for "mid-term" voltage stability and 1000, 10,000 s for "longer-term" voltage stability, using a ramp function equal to the linear increase in load demand.

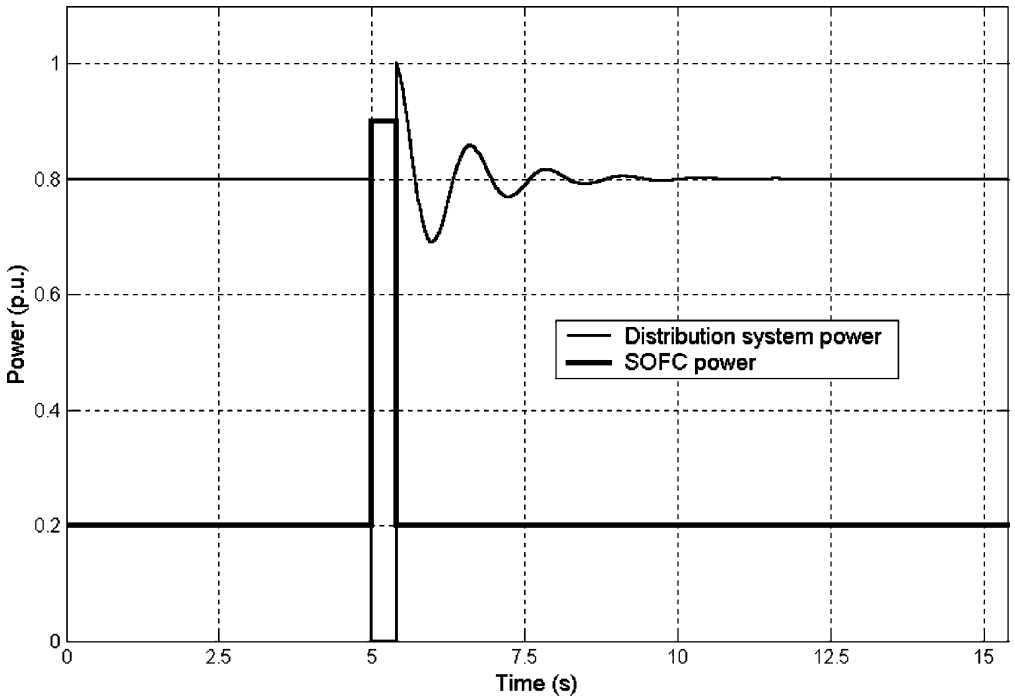


Fig. 6. Fast transient disturbances with inverter.

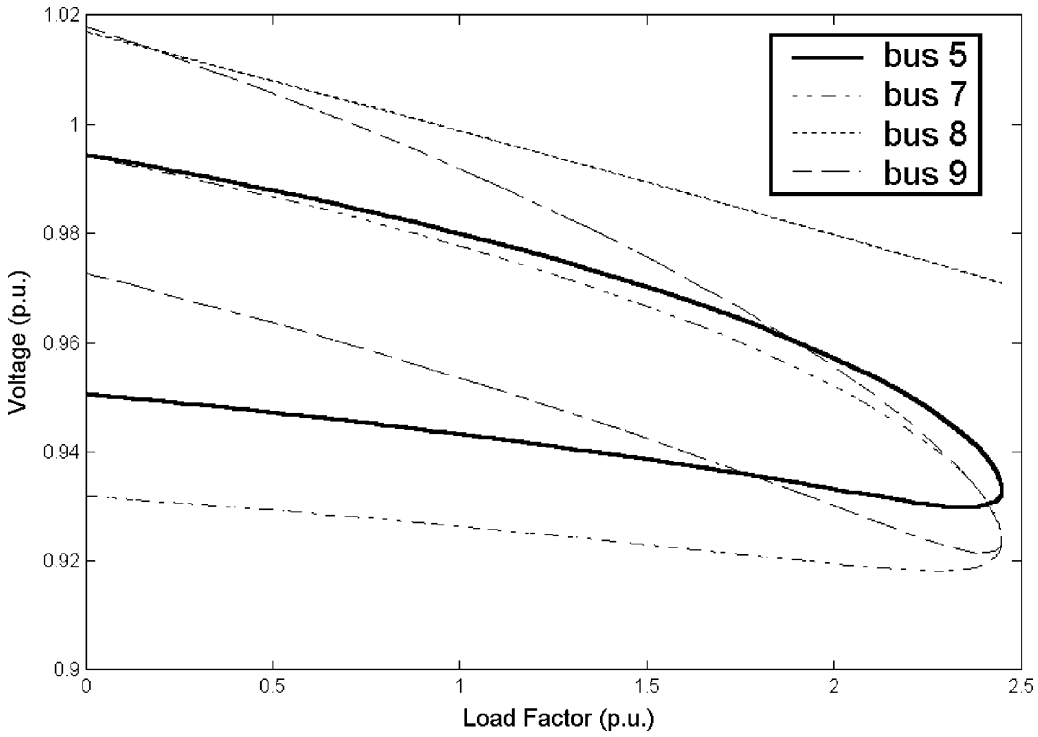


Fig. 7. Voltage profiles for the IEEE 13 bus test system.

The plant can contribute to the utility reactive power supply by continuously adjusting the set points $\psi_v^*$ of the inverter to regulate the magnitude of the interface bus voltage.

However, according to IEEE P1547, a SOFC system should trip offline if the magnitude of the local electric power system voltage falls below 88% for 2 s or 50% for 10 cycles.

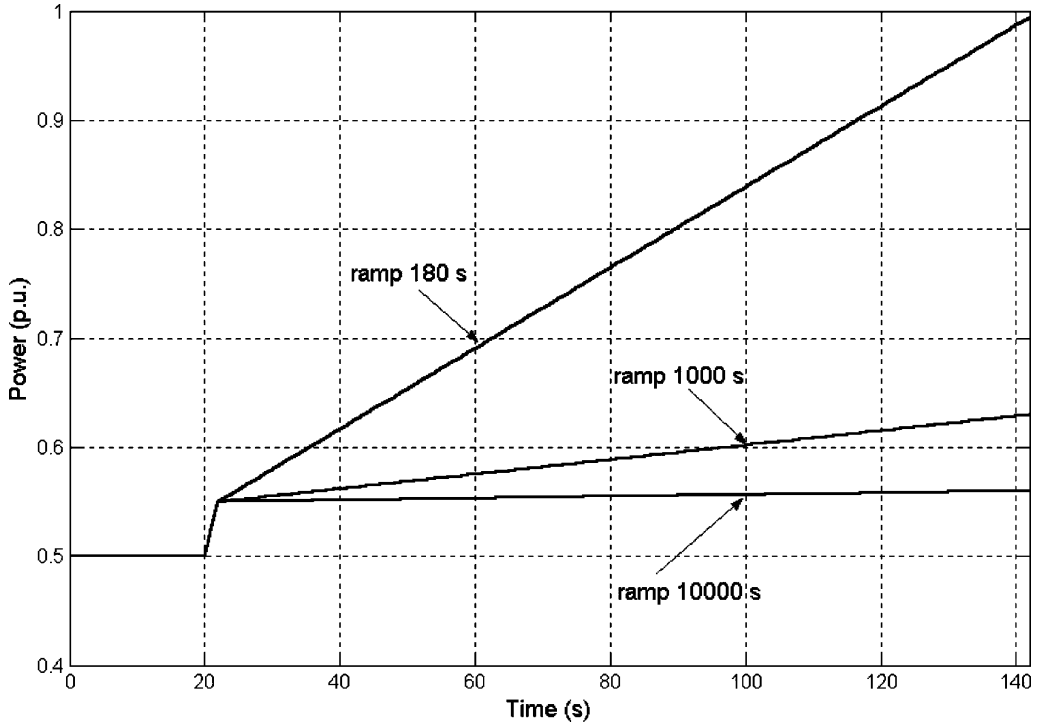


Fig. 8. Dynamic response of SOFC plant. Voltage instability at 180, 1000, and 10,000 s.

## 7. Conclusions

The introduction of SOFC within the context of an already existing grid can provide control of local bus voltage, control of base power flow thus reducing the power demand from the main grid feeder, and ultimately frequency control associated with load sharing within units located in the micro-grid.

The SOFC is capable of providing effective load-following service in the distribution system. However, the results also show that the SOFC system is not an uninterruptible power supply and does not protect the load from voltage stability while in grid-connect mode.

When SOFC plant is connected to a point where it gives support to a load in fault conditions, transient stability is enhanced with aid of the SOFC inverter.

## References

[1] T. Moore, Market potential high for fuel cells, EPRI J. 22 (3) (1997) 6–17.
[2] Scientific American, The Future of Fuel Cells, July 1999, pp. 72–83.
[3] N.F. Bessette, Modeling and Simulation for Solid Oxide Fuel Cell Power Systems, Ph.D. Thesis, Georgia Institute of Technology, 1994.
[4] C.L. Haynes, Simulation of Tubular Solid Oxide Fuel Cell Behavior for Integration Into Gas Turbine Cycles, Ph.D. Thesis, Georgia Institute of Technology, July 1999.
[5] J. Padullés, G.W. Ault, J.R. McDonald, An integrated SOFC plant dynamic model for power systems simulation, J. Power Sources 86 (1–2) (2000) 495–500.
[6] A.F. Massardo, F. Lubelli, Internal reforming solid oxide fuel cell-gas turbine combined cycles (IRSOFC-GT). Part A. Cell model and cycle thermodynamic analysis, J. Eng. Gas Turbines Power 122 (27) (2000) 27–35.
[7] S. Campanari, Thermodynamic model and parametric analysis of a tubular SOFC module, J. Power Sources 92 (1–2) (2001) 26–34.
[8] R. Lasseter, Dynamic models for micro-turbines and fuel cells, in: Proceedings of the IEEE/PES Summer Meeting, vol. 2, 2001, pp. 761–766.
[9] A.D. Rao, G.S. Samuelsen, Analysis strategies for tubular solid oxide fuel cell based hybrid systems, J. Eng. Gas Turbines Power 124 (3) (2002) 503–509.
[10] F. Jurado, Power supply quality improvement with a SOFC plant by neural-network-based control, J. Power Sources 117 (2003) 75–83.
[11] P.P. Barker, R.W. De Mello, Determining the impact of distributed generation on power systems. I. Radial distribution systems, in: Proceedings of the IEEE/ PES Summer Meeting, vol. 3, 2000, pp. 1645–1656.
[12] N.M. Ijumba, A.A. Jimoh, M. Nkabinde, Influence of distribution generation on distribution network performance, African IEEE 2 (1999) 961–964.
[13] J.-H. Choi, J.-C. Kim, Advanced voltage regulation method of power distribution systems interconnected with dispersed storage and generation systems, IEEE Trans. Power Delivery 16 (2) (2001) 329–334.
[14] E.W. Kimbark, Power System Stability, IEEE Press, New York, 1995.
[15] I.J. Nagrath, D.P. Kothari, Power System Engineering, McGraw-Hill, New Delhi, 1994.
[16] P. Kundur, Power System Stability and Control, EPRI Power System Engineering Series, McGraw-Hill, New York, 1994.
[17] P.W. Sauer, M.A. Pai, Power System Dynamics and Stability, Prentice-Hall, New Jersey, 1998.
[18] R. Patel, T.S. Bhatti, D.P. Kothari, Improvement of power system transient stability using fast valving a review, Electr. Power Components Syst. 29 (10) (2001) 927–938.
[19] C.W. Taylor, Power System Voltage Stability, New York, McGraw-Hill, 1994 (Chapter 2).
[20] C.A. Cañizares (Ed.), Voltage Stability Assessment: Concepts, Practices and Tools, Final Report, IEEE/PES Power Systems Stability Subcommittee Special Publication, 2002.
[21] C.A. Cañizares, F.L. Alvarado, Point of collapse and continuation methods for large ac/dc systems, IEEE Trans. Power Syst. 8 (1) (1993) 1–8.
[22] C.A. Cañizares, On bifurcations, IEEE Trans. Power Syst. 10 (1) (1995) 512–522.
[23] M.C. Chandorkar, New techniques for inverter flux control, IEEE Trans. Ind. Appl. 37 (3) (2001) 880–887.
[24] J.A. Kuipers, in: Proceedings of the 1998 Fuel Cell Seminar, 1998, p. 450.
[25] S.C. Singhal, Progress in tubular solid oxide fuel cell technology, in: Proceedings of the Solid Oxide Fuel Cells, Honolulu, HI, USA, 17–22 October 1999, pp. 39–51.
[26] M.K. Donnelly, J.E. Dagle, D.J. Trudnowski, G.J. Rogers, Impacts of the distributed utility on transmission system stability, IEEE Trans. Power Syst. 11 (2) (1996) 741–746.